

Chromatin patterns associated with lung adenocarcinoma progression

Brooke R. Druliner,¹ Justin A. Fincher,¹ Brittany S. Sexton,¹ Daniel L. Vera,¹ Michael Roche,² Stephen Lyle² and Jonathan H. Dennis^{1,*}

¹Department of Biological Science; Florida State University; Tallahassee, FL USA;

²Departments of Cancer Biology and Pathology; University of Massachusetts Medical School; Worcester, MA USA

Keywords: nucleosome, chromatin, lung, cancer, chromosome, adenocarcinoma, MNase, microarray, accessibility, genome

The development and progression of lung adenocarcinoma, one of the most common cancers, is driven by the interplay of genetic and epigenetic changes and the role of chromatin structure in malignant transformation remains poorly understood. We used systematic nucleosome distribution and chromatin accessibility microarray mapping platforms to analyze the genome-wide chromatin structure from normal tissues and from primary lung adenocarcinoma of different grades and stages. We identified chromatin-based patterns across different patients with lung adenocarcinoma of different cancer grade and stage. Low-grade cancers had nucleosome distributions very different compared with the corresponding normal tissue but had nearly identical chromatin accessibility. Conversely, nucleosome distributions of high-grade cancers showed few differences. Substantial disruptions in chromosomal accessibility were seen in a patient with a high-grade and high-stage tumor. These data imply that chromatin structure changes during the progression of lung adenocarcinoma. We have therefore developed a model in which low-grade lung adenocarcinomas are linked to changes in nucleosome distributions, whereas higher-grade tumors are linked to large-scale chromosomal changes. These results provide a foundation for the development of a comprehensive framework linking the general and locus-specific roles of chromatin structure to lung cancer progression. We propose that this strategy has the potential to identify a new class of chromatin-based diagnostic, prognostic and therapeutic markers in cancer progression.

Introduction

Since early in the last century, investigators have known that chromosome alterations can lead to cancer.¹ In fact, a hallmark of the transformed phenotype is altered chromosome structure, and important studies have identified many chromosomal aberrations used to mark cancer type.² Studies at the molecular level have shown that these transformation events are driven by the interplay of genetic and epigenetic changes.^{3,4} Specifically, large chromosomal changes have been observed in different cancers, and susceptibility of gene loci, losses and gains and translocations have been identified at specific chromosomes.⁵⁻¹⁰

The progression of lung adenocarcinoma (LAC) can be classified by histopathological grade and tumor stage. Tumors of different grades can be distinguished by their gene expression profiles, and gene expression changes are thought to be driven by tumor grade.^{11,12} Studies have also revealed a correlation between tumor stage and mutations at specific genes.¹³ Beyond the analysis of specific gene loci in the context of tumor grade and stage, documentation of the genetic or epigenetic basis for the progression of cancer is insufficient. As chromosomal aberrations are well documented in nearly all cancers, the currently limited information on the role of chromatin structure in the progression of LAC is surprising. Moreover, although numerous studies have addressed

chromosomal aberrations in cancer, broad assessment of the underlying structure of chromatin has been understudied, and its role in malignant transformation remains poorly characterized.

Understanding the functional organization of the genome remains one of the biggest challenges in biology. Eukaryotic genomes consist of DNA that is packaged together with histone proteins into chromatin. The basic subunit of chromatin is the nucleosome, which is composed of approximately 150 base pairs of DNA wrapped 1.65 times around a histone octamer.¹⁴ The distribution of nucleosomes is controlled by a combination of chromatin regulatory complexes and features intrinsic to DNA sequence. This organization results in architectures that facilitate or impede DNA-binding interactions required for nuclear processes, such as transcription, replication, recombination, repair and transposition.¹⁵ The higher-order structure of chromatin is not well characterized despite its central importance to myriad genomic processes.¹⁶ Knowledge of nucleosome distribution and chromatin accessibility provides a critically important point of reference for interpreting epigenetic modification and high-order structures in diseases such as cancer.¹⁷⁻¹⁹

Systematic analysis of chromatin structure has provided insights into the mechanism behind chromosome alterations. A classic method for analysis of chromatin structure first described more than 25 years ago uses nuclease sensitivity as a probe of

*Correspondence to: Jonathan Dennis; Email: dennis@bio.fsu.edu
Submitted: 04/09/13; Accepted: 04/11/13
<http://dx.doi.org/10.4161/cc.24664>

highly diffusible molecules.²⁰ This assay remains a powerful method for measuring changes in higher-order chromatin structure and has been enhanced by use in combination with modern genomic tools. Recent advances in microarray technology have facilitated application of this classic assay to scales at multiple levels of resolution across the entire genome, where nuclease was used as a probe for determining inaccessible and accessible regions of the genome. We have used a systematic analysis of chromatin structural information for lung cancer progression to seek a better understanding of cancer etiology.^{19,21,22}

Our work indicates that there is an association between chromatin structure and the progression of cancer. We have shown this link through the analysis of chromatin structure of LAC patients of different grades and stages at two scales: nucleosome distribution and chromatin accessibility. Furthermore, we have been able to identify discrete chromatin-based patterns that are consistent with different grades of cancer.

Results

Identification of the nucleosome distribution changes in lung adenocarcinoma. To investigate the role of chromatin structure in the progression of LAC, we sought to determine if changes in nucleosome distribution were a feature of LAC. We used a microarray-based assay to analyze primary LAC tumors and their corresponding normal tissue from multiple patients. To analyze nucleosome distribution, we isolated mononucleosomally protected DNA from MNase-digested chromatin of both tumor and normal tissue from each patient. Using microarrays containing 886 transcription start sites of cancer and immunity-related genes (Fig. 1A), we were able to detect changes in nucleosome distribution between tumor and normal, for each patient. We devised a systematic and unbiased statistical method (using a sliding window t-test) for comparing differences between the normal and tumor tissue for each patient.

Low-grade tumor samples show many changes in nucleosome distribution. To assess the role nucleosome distribution plays in cancer progression, we clustered the patient samples on the basis of histopathological grade, and found that low-grade tumors showed many changes in nucleosome distribution. We defined changes using a sliding window t-test across the 2,000 bp surrounding the transcription start site of each of 886 genes, and if the overall t-test mean was above a significance threshold, the nucleosome distribution at that gene was considered significantly changed. The nucleosome distribution in the tumor and corresponding normal tissue differed at an average of 446 of 886 (50%) genes in the grade 1 samples, 57 (6%) genes in the grade 2 samples and 158 (18%) genes in the grade 3 samples (Fig. 1B). We were particularly struck by the number of differences in nucleosome distribution seen in the grade 1 patients: #1357 (633 genes) and #4137 (490 genes). In addition, the differences between normal vs. tumor at each probe for all genes are shown as boxplots for two grade 1 patients (#1357 and #4137) and two grade 3 patients (#873 and #386), showing that the range of differences in the grade 1 patients is much broader (Fig. 1C). Correlation plots are shown between normal data and normal data, grade 1 data and

grade 3 data (Fig. 1D, from left to right). The Spearman's rank correlation coefficient is shown in each of the plots; the normal-normal and grade 3-normal coefficients are both ~ 0.9 , but the grade 1-normal coefficient is lower, at 0.78, consistent with the many changes in nucleosome distribution for grade 1 tumors.

The nucleosome distribution plots for the ATM gene, a highly mutated gene in LAC,¹³ are shown in plots of normal compared with normal, grade 1 and grade 3 data (Fig. 1E, from left to right). These plots show that normal lung epithelial tissue from a patient has a similar nucleosome distribution to both a normal tissue from a different patient and to a high-grade LAC tumor, but a normal tissue compared to a grade 1 LAC shows multiple changes, including a complete loss of a nucleosome. Altogether, these results suggest that the molecular pathology of lower grade LAC is defined by nucleosome distribution change at specific gene loci.

Nucleosome distribution changes in low-grade tumors at LAC-specific gene loci. We next wanted to see if nucleosome distribution changes in grade 1 tumors occurred at genes previously reported in the literature as being implicated in LAC, and if the changes were consistent between patients with tumors of the same grade. In order to visualize nucleosome distribution changes, we have shown nucleosome distribution plots for five genes selected from the 446 genes showing changes grade 1 LAC patients, which are reported as being cancer-related, two of which are specific to LAC carcinogenesis: ATM, MYC, RHOC, ITGA4 and MLL5 (Fig. 2A–E). The grade 1 tumor samples (red lines) show changes in nucleosome distribution compared with normal samples (black lines) for all genes here, whereas grade 3 tumor samples do not. In each case, the gene loci that showed the greatest differences in the grade 1 patients shared an overall depletion of nucleosomes, suggesting a common mechanism of chromatin regulation in LAC.

Nucleosome distribution changes are consistent between patients. Importantly, changes in nucleosome distribution for grade 1 samples are consistent between different patients (Fig. 2A–E). We were able to identify patterns of nucleosome-distribution changes consistent between and unique to the grade 1 tumors (Fig. 2A–E, “grade 1” column). In a majority of cases we found that nucleosome distribution changes at particular genes in grade 1 samples were similar. Grade 2 and grade 3 tumor samples rarely deviated from the nucleosome distribution pattern seen in normal tissue (Fig. 2A–E, “grade 3” column). We compared the loci from grade 1 patients, and found that 168 of the 446 genes with altered nucleosome distribution were shared in common between patients (Fig. 2F). Gene ontology analysis showed that these shared genes were enriched for the regulation of the phosphoinositide 3-kinase (PI3K) cascade.

Identification of the chromatin accessibility changes in LAC. To investigate high-order chromatin structure in the progression of LAC, we determined if global chromosomal architecture was consistent with the trend we saw with nucleosome distribution experiments. Using a novel chromatin accessibility assay, where we isolated inaccessible and accessible fractions of the genome (Fig. 3A) from the same material used for the nucleosome distribution experiments, we were able to map changes in

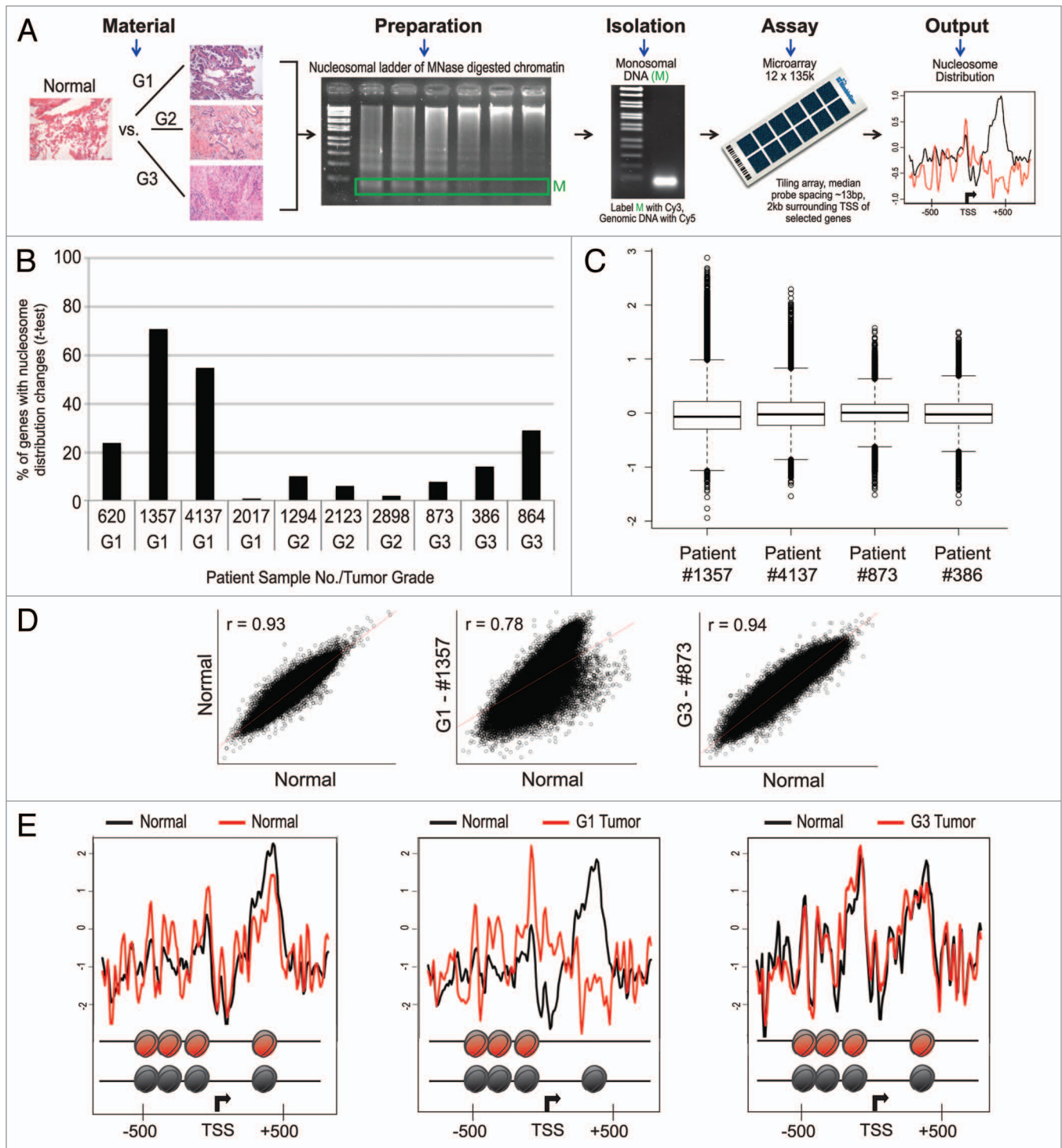


Figure 1. Low-grade tumor samples show many changes in nucleosome distribution. (A) A flowchart of the general method used to determine nucleosome distribution from primary lung tissue. Snap-frozen tissue from clinically resected lung adenocarcinomas of different grades and matched, normal lung epithelium were digested with a titration of MNase and resolved on an agarose gel. Mononucleosomes were gel purified and labeled with Cy3, and bare genomic DNA was extracted from the same tissue labeled with Cy5. Samples were hybridized to tiling transcription start site (TSS) microarrays, and the data plotted in R. (B) Percentage of genes out of 866 with the greatest nucleosome-distribution differences between normal and tumor tissue for each patient, determined by t-test. (C) Box plot of the differences between normal and tumor tissue for two grade 1 patients, #1357 and #4137, and two grade 3 patients, #873 and #386. (D) Scatterplot with correlation line and R-value for normal data plotted against (from left to right) normal data, grade 1 tumor data and grade 3 tumor data. (E) Read-out from microarray of the ATM gene for normal tissue vs. (from left to right) normal tissue (black) plotted against normal tissue, grade 1 tumor tissue and grade 3 tumor tissue (red lines). The x-axis represents a 2-kb range of genomic position centered on a TSS. Inferred nucleosomes are represented graphically (black ovals represent normal tissues; red ovals, tumor tissues). The y-axis is the log ratio of nucleosomal to bare genomic signal at each probe on the microarray.

chromatin accessibility. A 1 Mb non-overlapping sliding window t-test revealed regions across the genome in which each tumor sample and its corresponding normal tissue differed. The genome included approximately 1,660 nonoverlapping 1 Mb regions, in which resolution of the microarray (12.5 kb) and the number of probes within each window were taken into account. When the regions that changed were clustered according to cancer grade, we did not see the same trend as in the nucleosome-distribution experiments (Fig. 3B). Instead, we found that no tumor samples showed many regions of change in chromatin accessibility, except for a single grade 3 sample, #873. Clustering the patient samples by stage revealed that patient #873, who had the highest percentage of regions changed, was also at the highest LAC stage, IIB.

The chromatin-accessibility plots are consistent with statistical analysis, in which the tumor samples are indistinguishable from normal samples, with modest variations (specifically patient #620, modest variation which can account for the higher percentage of regions changed compared with other samples). In patient #873, large-scale, catastrophic changes in accessibility were observed (Fig. 3C). When the normal tissue from five patients were examined, the plots were indistinguishable from each other, with scarce variation, confirming the sensitivity of this assay (Fig. 3D).

Discussion

In the present study, we analyzed the nucleosome distribution at the transcription start sites of 886 genes and genome-wide chromatin accessibility of tumors from LAC patients with matched normal tissue. Surprisingly, we found: (1) a majority of genes studied showed significant nucleosome distribution changes; (2) nucleosome distribution changes are limited to low-grade tumors and are not observed in high-grade tumors; (3) nucleosome distribution changes are consistent between different patients and (4) global chromatin accessibility profiles show catastrophic changes in aggressive tumors. Our results argue strongly for the importance of chromatin structure in the progression of cancer.

We present the first identification of nucleosome distribution changes between tumor and matched normal primary patient tissue in LAC. We found that of the 886 genes studied, we were able to detect changes in the majority of genes. Furthermore, we found that nucleosome distribution changes in the majority of genes occur in low-grade tumors, while no changes were evident in high-grade tumors. In fact, nucleosome distribution changes appear to potentiate early transformation events, due to the finding that changes were observed only in low-grade tumors.

The mechanism by which nucleosome distribution changes in low-grade LAC tumors contribute to or permit the progression to more aggressive tumor is unclear, but our findings are consistent with a critical role for chromatin structural alterations as an early transformation event. Importantly, nucleosome distribution changes in low-grade tumors are concordant between patients, pointing to a shared regulatory mechanism that drives the changes. One attractive explanation involves ATP-dependent chromatin remodelers, which are responsible for altering the positions and density of nucleosomes with respect to the underlying

DNA sequence. Recent data from exome sequencing in matched normal and tumor patient samples have shown chromatin remodelers to be frequently mutated in multiple cancers.^{23,24} In addition, subunits of the chromatin remodeler SWI/SNF complex can act as tumor suppressors in cancer; specifically, loss of BRG1 and BRM expression has been reported as an indicator of poor prognosis in non-small-cell lung cancer.^{25,26} Our data suggest that the observed nucleosome distribution changes are an early, regulated transformation event governed by chromatin remodelers.

The genomic loci showing measurable differences in nucleosome distribution in the low-grade samples are enriched for genes involved in the PI3K pathway. Activation of this signaling network commonly occurs in human tumors through mutation of the components involved in the pathway and has been specifically implicated in LAC.^{13,27,28} The pathway is activated by growth factors, which activate RAS through receptor tyrosine kinases, leading to stimulation of the PI3K pathway and other pathways involved in the control of cellular growth, proliferation and survival. Studies have successfully used PI3K-inhibitory drugs in transgenic mouse models to block the growth of lung tumors.²⁹ In addition, clinical trials involving small molecular inhibitors of PI3K have recently begun,²⁷ indicating the importance of this pathway as a potential cancer therapy. If changes in nucleosome distribution act as an early indicator of impending gene-expression changes, then our nucleosome-distribution measurements could act as predictive indicators of early transformation events in this key oncogenetic pathway.

By contrast to nucleosome distribution experiments, global chromatin accessibility experiments for the same patients do not show the same trend. In fact, low-grade tumors did not differ from normal tissues in chromatin accessibility, except in a high-grade, high-stage tumor, where extreme chromatin accessibility changes across the entire genome were observed. A recent study has revealed that in 2–3% of different cancer types, including lung cancer, a single cellular crisis event called chromothripsis occurs, in which tens to hundreds of chromosome rearrangements are acquired.²⁸ Our measurements of substantial chromosomal accessibility alterations in the high-grade, high-stage tumor is consistent with a chromothripsis event. Our results might well reflect the pathology of chromothripsis and the role it may play in cancer progression.

While screening and diagnostic methods have been identified for some cancers (e.g., breast, cervical, prostate), robust indicators have not been identified for lung cancer. In fact, the long-term survival rate for patients with lung cancer remains low, and molecular markers that have been identified to date are unsuitable for clinical trials.^{30,31} The identification of nucleosome distribution and chromatin accessibility profiles provides a new set of genotype-independent and gene expression-independent measurements with which to classify LAC. In our samples we were able to identify nucleosome distribution changes common to all grade 1 LAC, as well as patient-specific nucleosome distribution changes. Likewise we identified catastrophic chromosomal changes in aggressive LAC. These data have allowed us to develop a model in which early-grade lung adenocarcinomas are linked to changes in nucleosome distributions, while later-grade

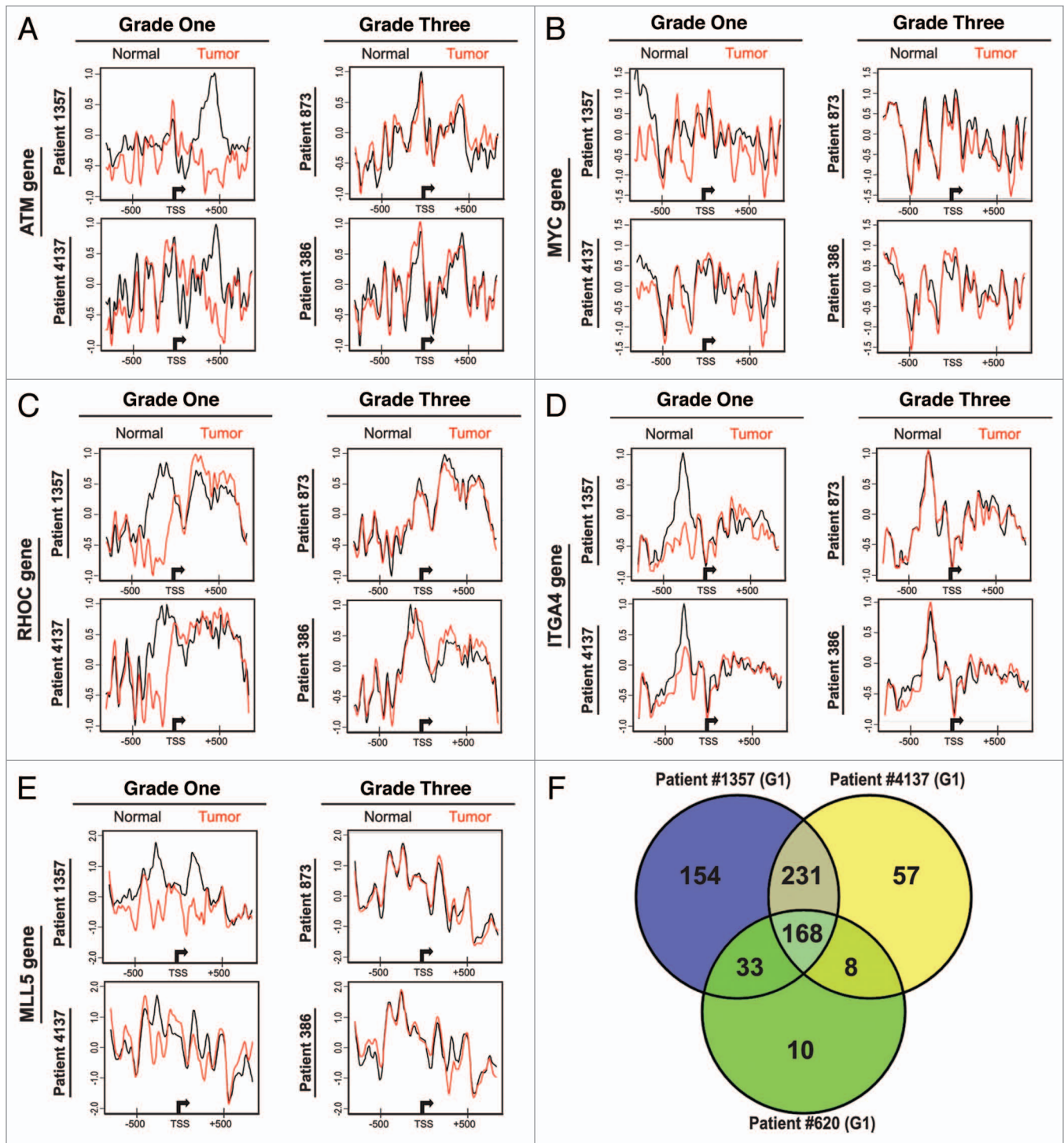


Figure 2. Consistency of nucleosome distribution changes for key cancer-related genes between patients. The nucleosome distribution for normal tissue (black lines) and tumor tissue (red lines) from four patients with grade 1 tumors (#1357 and #4137) and grade 3 tumors (#873 and #386) for five genes implicated in lung adenocarcinoma and in cancer in general: (A) ATM (seen previously in Fig. 1), (B) MYC, (C) RHOC, (D) ITGA4 and (E) MLL5. The x-axis represents a 2-kb range of genomic position centered on a transcription start site. The y-axis is the log ratio of nucleosomal to bare genomic signal at each probe on the microarray. (F) 168 genes with the highest percentages of nucleosome-distribution changes are shared by grade 1 patients and are enriched for the regulation of the PI3K cascade. G1, grade 1.

cancers are linked to large-scale chromosomal changes (Fig. 4). Further analysis of the chromatin structural changes presented in this work may provide new explanations of the etiology of early

and late transformation events. Finally, these chromatin structural profiles have the potential to serve as potent objective diagnostic and prognostic tools to be used in the determination of

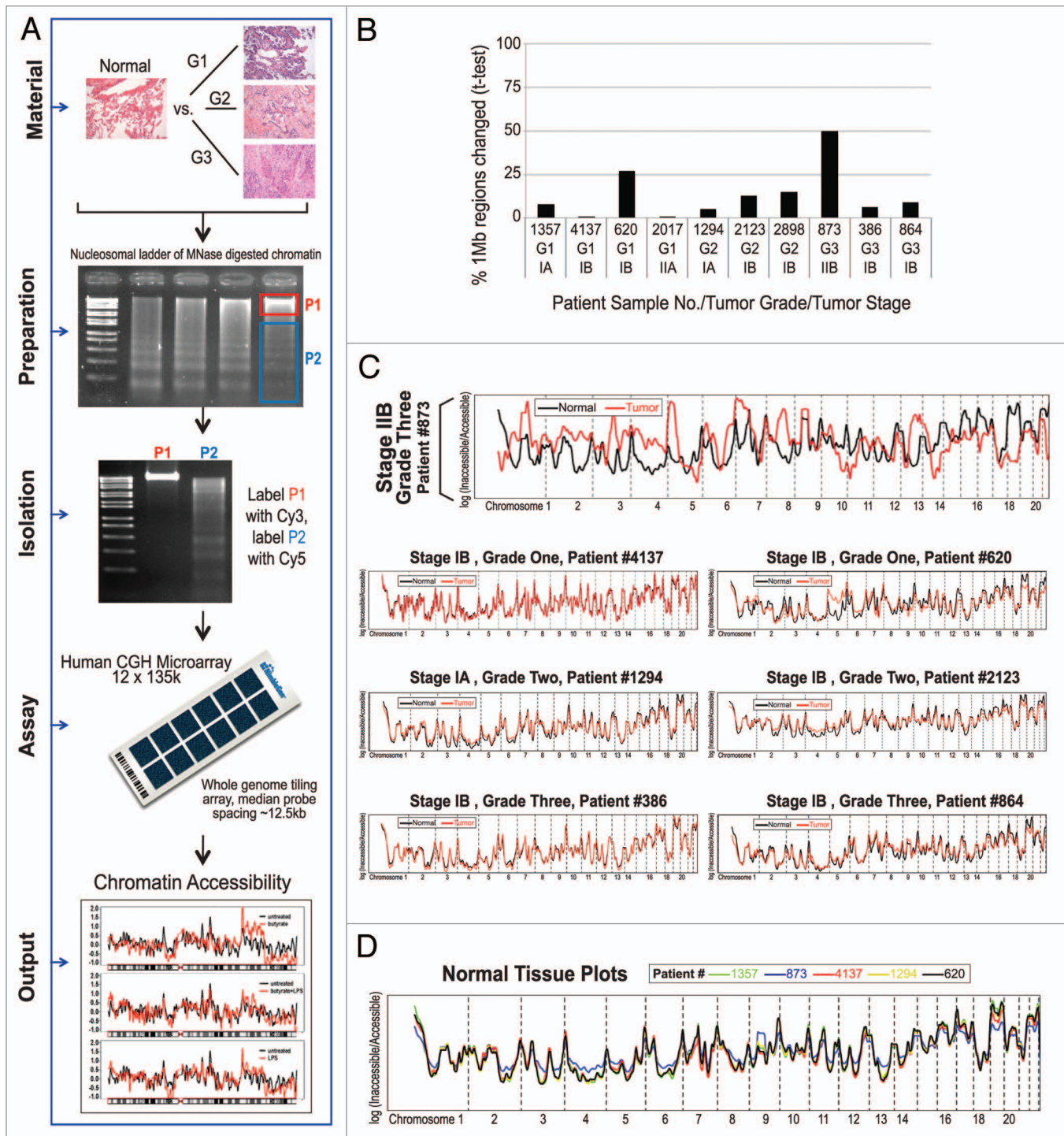


Figure 3. High-grade, high-stage tumors show major changes in chromatin accessibility. **(A)** A flowchart of the general method used to determine chromatin accessibility from primary lung tissue. The samples were identical to those used for the nucleosome distribution experiments. A single concentration of MNase from the titration generated previously was selected, and high-molecular-weight and low-molecular-weight fractions (corresponding to inaccessible and accessible regions of chromatin, respectively) were gel purified. Inaccessible fractions were labeled with Cy3 and accessible fractions with Cy5. Both were hybridized to a tiling microarray spanning the entire genome with probes spaced every 12.5 kb, and the data were plotted in R. **(B)** Percentage of regions in which normal and tumor tissue for each patient differed according to 1-MB t-test windows spanning the entire genome. **(C)** Chromatin accessibility read-out for seven patients representing different grades and stages is shown. The top plot is the high-grade, high-stage tumor sample, which shows massive changes in accessibility across the genome. The remaining six plots show no accessibility changes but modest variation at chromosome 5 in patient #620. The x-axis represents genomic position; dotted vertical lines indicate chromosome start/stop. The y-axis is the log ratio of inaccessible to accessible signal at each probe on the microarray. The 23 autosomes are plotted; black line, normal; red line, tumor. **(D)** The normal tissues for five patients are plotted simultaneously, showing that differences between normal lung epithelium tissues from isogenic patients are very modest.

appropriate therapies for patients. This work represents an important first step in the identification of an entirely new class of chromatin structural biomarkers that will pave the way for similar detailed studies of the role of chromatin structure across multiple cancer types.

Methods

Patient tissue. Primary samples from LAC patients with a surgically removed tumor, and matched normal tissue were selected from the University of Massachusetts Medical School Tissue Bank (Table S1). The tumor and normal material was snap frozen in liquid nitrogen within 1 h of surgery. Patient samples were examined by Dr Stephen Lyle, using hematoxylin and eosin staining. Only samples with 80% or more tumor cells were included, as assessed by histological examination. Patient samples were anonymized, and we received patient history along with the samples.

Tissue processing and nuclei purification. Snap-frozen patient biopsy samples were shipped from the tissue bank lab overnight on dry ice. Samples arrived as approximately 3 mm³ blocks of frozen tissue weighing between 400–600 mg. Samples were pulverized in a mortar and pestle in liquid nitrogen. For all microarray studies, ~90% of the resulting powder was cross-linked in 1% formaldehyde in PBS for 10 min at RT, and nuclei were extracted in nuclei isolation buffer (0.3 M sucrose, 2 mM MgOAc₂, 1 mM CaCl₂, 1% Nonidet P-40, 10 mM HEPES, pH 7.8) and dounce-homogenized. 10% of the pulverized tissue sample was used for isolation of total bare genomic DNA for use as reference in nucleosome distribution experiments. All samples were flash frozen and stored at –80°C, until all samples were ready to be processed in parallel. We were able to isolate enough material to run replicates of a selection of our experimental assays.

MNase cleavage, mononucleosomal purification and fluorescent labeling for nucleosome distribution. Ground tissue from the primary LAC tumors and matched normal tissue were digested with titrated amounts of MNase (Worthington Biochemical Corp.) for nucleosome distribution experiments. Nucleosome distribution protocols were performed as previously described.³² An MNase titration reaction of 10 U/ml, 5 U/ml, 2.5 U/ml and 1.25 U/ml MNase in MNase cleavage buffer (4 mM CaCl₂, 25 mM KCl, 4 mM MgCl₂, 12.5% glycerol, 50 mM Hepes, pH 7.8) was performed for 5 min at 37°C, and stopped with 50 mM EDTA. MNase-digested nuclei were then treated with proteinase K to a final concentration of 0.2 µg/µl, sodium dodecyl sulfate (SDS) to a final concentration of 1%, and the cross-links were reversed by overnight incubation at 65°C. DNA was purified by performing a phenol/chloroform extraction. The aforementioned steps were repeated for each concentration of MNase, and each set of samples for nucleosome distribution experiments.

To isolate mononucleosomal DNA for the nucleosome distribution DNA microarrays (test sample), the nucleosomal ladder was resolved on a 2% agarose gel, and the mononucleosomal DNA band (~150 bp) was excised across all MNase concentrations and

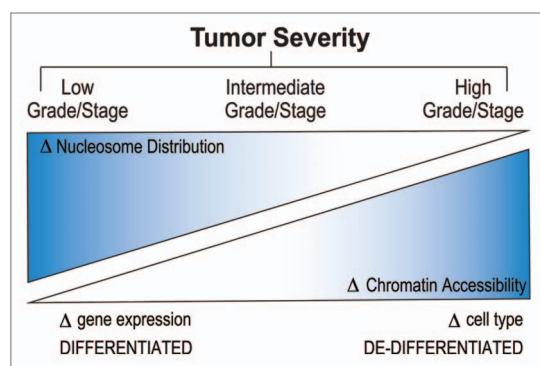


Figure 4. An initial model for chromatin structural patterns of cancer progression. We have developed an initial model for tumor progression in lung adenocarcinoma and potentially cancer in general. In this model, well-differentiated tumors are characterized by many changes in nucleosome distribution at key genes involved in oncogenic pathways. Additionally, chromatin accessibility changes are characteristic of an aggressive tumor type. Chromatin structure-based classification of tumors may be critical in determining appropriate, targeted therapy.

purified by electroelution. The mononucleosomal band should be cut across several titrations to ensure equal representation of the genome. To prepare the total bare genomic DNA from tumor and normal samples (reference sample), we isolated genomic DNA from the ground tissue by resuspending in a 1% SDS and 0.2 µg/µl proteinase K solution, incubated overnight at 55°C and phenol/chloroform extracted DNA.

We used the NimbleGen protocol to label material for all microarrays. A fluorescently labeled random 7-mer oligonucleotide primer was used in a Klenow fill-in reaction to label the mononucleosomally protected and bare genomic reference DNA samples. The mononucleosomally protected DNA sample was labeled with a fluorescently labeled Cy3 primer, and reference total bare genomic DNA was labeled with a fluorescently labeled Cy5 primer. One microgram of sample was used for each labeling reaction. The labeling materials, labeling procedure and hybridization protocols can be obtained from the array manufacturer.

Microarray design. We used the NimbleGen platform for all microarray experiments. For nucleosome distribution experiments, we utilized two custom designed high-resolution DNA microarrays. Each of these microarrays cover 2,000 bp flanking the TSSs of either (1) 414 cancer-related genes or (2) 472 inflammation- and immunity-related genes, selected based on publications on their functional relevance to cancer or the innate immune response (Table S2 and S3). The TSS sequences were repeat masked, so only unique probes were printed on the microarray. Both forward and reverse strands were tiled on the microarray to provide experimental redundancy and account for strand-specific effects. The 60-mer oligonucleotide probes were tiled with an average 13 bp spacing (47 bp overlap). Each of the 12 subarrays on the microarray contained approximately 135,000 60-mer unique and isothermal oligonucleotide probes. We used NimbleGen HD2 design (2.1 million features per microarray), 12-plex (12 individual isolated experiments per microarray) custom-designed and commercially available microarrays, including

built in replicates for controls. The 12-plex format allowed for 135,000 oligonucleotide probes to be queried in each experiment.

Microarray data, statistical analysis and computational model. We have developed several computational tools for the analysis of microarray data. Our lab developed software specifically designed for the analysis of nucleosome distribution microarray data. This software, drawGff, runs in the R environment for statistical computing and graphical output. Our software contains a variety of statistical, graphical plotting and comparative analysis tools designed to identify important features within and across microarray data sets. Specifically, the output of the microarray was a \log_2 ratio of the Cy3 and Cy5 inputs. Data sets were normalized by standard score normalization, and smoothing was accomplished by LOESS. Scores were computed on non-overlapping consecutive windows, and probes were assigned to

windows based on the probe start coordinate. The t-test mean at each TSS (nucleosome distribution) was calculated to determine changes between tumor and matched normal.

Our software will continue to be developed and is freely available to the public, including tutorial and help pages (<http://chromatin.bio.fsu.edu>). All data sets and additional supporting analyses presented in the results are available at (http://chromatin.bio.fsu.edu/Drulineretal_2013a).

Disclosure of Potential Conflicts of Interest

No potential conflicts of interest were disclosed.

Supplemental Materials

Supplemental materials may be found here: www.landesbioscience.com/journals/cc/article/24664

References

1. Knudson AG. Cancer genetics. *Am J Med Genet* 2002; 111:96-102; PMID:12124744; <http://dx.doi.org/10.1002/ajmg.10320>
2. Hanahan D, Weinberg RA. The hallmarks of cancer. *Cell* 2000; 100:57-70; PMID:10647931; [http://dx.doi.org/10.1016/S0092-8674\(00\)81683-9](http://dx.doi.org/10.1016/S0092-8674(00)81683-9)
3. Risch A, Plass C. Lung cancer epigenetics and genetics. *Int J Cancer* 2008; 123:1-7; PMID:18425819; <http://dx.doi.org/10.1002/ijc.23605>
4. Sharma S, Kelly TK, Jones PA. Epigenetics in cancer. *Carcinogenesis* 2010; 31:27-36; PMID:19752007; <http://dx.doi.org/10.1093/carcin/bgp220>
5. Hayashi N, Sugimoto Y, Tsuchiya E, Ogawa M, Nakamura Y. Somatic mutations of the MTS (multiple tumor suppressor) 1/CDK4l (cyclin-dependent kinase-4 inhibitor) gene in human primary non-small cell lung carcinomas. *Biochim Biophys Res Commun* 1994; 202:1426-30; PMID:8060323; <http://dx.doi.org/10.1006/bbrc.1994.2090>
6. Landi MT, Chatterjee N, Yu K, Goldin LR, Goldstein AM, Rotunno M, et al. A genome-wide association study of lung cancer identifies a region of chromosome 5p15 associated with risk for adenocarcinoma. *Am J Hum Genet* 2009; 85:679-91; PMID:19836008; <http://dx.doi.org/10.1016/j.ajhg.2009.09.012>
7. Li Y, Sheu CC, Ye Y, de Andrade M, Wang L, Chang SC, et al. Genetic variants and risk of lung cancer in never smokers: a genome-wide association study. *Lancet Oncol* 2010; 11:321-30; PMID:20304703; [http://dx.doi.org/10.1016/S1470-2045\(10\)70042-5](http://dx.doi.org/10.1016/S1470-2045(10)70042-5)
8. Liu P, Vikis HG, Lu Y, Wang Y, Schwartz AG, Pinney SM, et al. Cumulative effect of multiple loci on genetic susceptibility to familial lung cancer. *Cancer Epidemiol Biomarkers Prev* 2010; 19:517-24; PMID:20142248; <http://dx.doi.org/10.1158/1055-9965.EPI-09-0791>
9. Sato M, Takahashi K, Nagayama K, Arai Y, Ito N, Okada M, et al. Identification of chromosome arm 9p as the most frequent target of homozygous deletions in lung cancer. *Genes Chromosomes Cancer* 2005; 44:405-14; PMID:16114034; <http://dx.doi.org/10.1002/gcc.20253>
10. Wang Y, Broderick P, Webb E, Wu X, Vijaykrishnan J, Matakidou A, et al. Common 5p15.33 and 6p21.33 variants influence lung cancer risk. *Nat Genet* 2008; 40:1407-9; PMID:18978787; <http://dx.doi.org/10.1038/ng.273>
11. Garber ME, Troyanskaya OG, Schluens K, Petersen S, Thaesler Z, Pacyna-Gengelbach M, et al. Diversity of gene expression in adenocarcinoma of the lung. *Proc Natl Acad Sci USA* 2001; 98:13784-9; PMID:11707590; <http://dx.doi.org/10.1073/pnas.241500798>
12. Neumann J, Feuerhake F, Kayser G, Wiech T, Aumann K, Passlick B, et al. Gene expression profiles of lung adenocarcinoma linked to histopathological grading and survival but not to EGF-R status: a microarray study. *BMC Cancer* 2010; 10:77; PMID:20196851; <http://dx.doi.org/10.1186/1471-2407-10-77>
13. Ding L, Getz G, Wheeler DA, Mardis ER, McLellan MD, Cibulskis K, et al. Somatic mutations affect key pathways in lung adenocarcinoma. *Nature* 2008; 455:1069-75; PMID:18948947; <http://dx.doi.org/10.1038/nature07423>
14. Kornberg RD, Lorch Y. Twenty-five years of the nucleosome, fundamental particle of the eukaryote chromosome. *Cell* 1999; 98:285-94; PMID:10458604; [http://dx.doi.org/10.1016/S0092-8674\(00\)81958-3](http://dx.doi.org/10.1016/S0092-8674(00)81958-3)
15. Jiang C, Pugh BF. Nucleosome positioning and gene regulation: advances through genomics. *Nat Rev Genet* 2009; 10:161-72; PMID:19204718; <http://dx.doi.org/10.1038/nrg2522>
16. Lanctôt C, Cheutin T, Cremer M, Cavalli G, Cremer T. Dynamic genome architecture in the nuclear space: regulation of gene expression in three dimensions. *Nat Rev Genet* 2007; 8:104-15; PMID:17230197; <http://dx.doi.org/10.1038/nrg2041>
17. Barski A, Cuddapah S, Cui K, Roh TY, Schones DE, Wang Z, et al. High-resolution profiling of histone methylations in the human genome. *Cell* 2007; 129:823-37; PMID:17512414; <http://dx.doi.org/10.1016/j.cell.2007.05.009>
18. Bernstein BE, Kamal M, Lindblad-Toh K, Bekiranov S, Bailey DK, Huebert DJ, et al. Genomic maps and comparative analysis of histone modifications in human and mouse. *Cell* 2005; 120:169-81; PMID:15680324; <http://dx.doi.org/10.1016/j.cell.2005.01.001>
19. Dennis JH, Fan HY, Reynolds SM, Yuan G, Meldrim JC, Richter DJ, et al. Independent and complementary methods for large-scale structural analysis of mammalian chromatin. *Genome Res* 2007; 17:928-39; PMID:17568008; <http://dx.doi.org/10.1101/gr.5636607>
20. Weintraub H, Groudine M. Chromosomal subunits in active genes have an altered conformation. *Science* 1976; 193:848-56; PMID:948749; <http://dx.doi.org/10.1126/science.948749>
21. Oszolák F, Song JS, Liu XS, Fisher DE. High-throughput mapping of the chromatin structure of human promoters. *Nat Biotechnol* 2007; 25:244-8; PMID:17220878; <http://dx.doi.org/10.1038/nbt1279>
22. Yuan GC, Liu YJ, Dion MF, Slack MD, Wu LF, Altschuler SJ, et al. Genome-scale identification of nucleosome positions in *S. cerevisiae*. *Science* 2005; 309:626-30; PMID:15961632; <http://dx.doi.org/10.1126/science.1112178>
23. Varela I, Tarpey P, Raine K, Huang D, Ong CK, Stephens P, et al. Exome sequencing identifies frequent mutation of the SWI/SNF complex gene PBRM1 in renal carcinoma. *Nature* 2011; 469:539-42; PMID:21248752; <http://dx.doi.org/10.1038/nature09639>
24. Wiegand KC, Shah SP, Al-Agha OM, Zhao Y, Tse K, Zeng T, et al. ARID1A mutations in endometriosis-associated ovarian carcinomas. *N Engl J Med* 2010; 363:1532-43; PMID:20942669; <http://dx.doi.org/10.1056/NEJMoa1008433>
25. Neely KE, Workman JL. The complexity of chromatin remodeling and its links to cancer. *Biochim Biophys Acta* 2002; 1603:19-29; PMID:12242108
26. Reisman DN, Sciarrotta J, Wang W, Funkhouser WK, Weissman BE. Loss of BRG1/BRM in human lung cancer cell lines and primary lung cancers: correlation with poor prognosis. *Cancer Res* 2003; 63:560-6; PMID:12566296
27. Marone R, Cmijlanovic V, Giese B, Wymann MP. Targeting phosphoinositide 3-kinase: moving towards therapy. *Biochim Biophys Acta* 2008; 1784:159-85; PMID:17997386; <http://dx.doi.org/10.1016/j.bbapap.2007.10.003>
28. Stephens PJ, Greenman CD, Fu B, Yang F, Bignell GR, Mudie LJ, et al. Massive genomic rearrangement acquired in a single catastrophic event during cancer development. *Cell* 2011; 144:27-40; PMID:21215367; <http://dx.doi.org/10.1016/j.cell.2010.11.055>
29. Engelman JA, Chen L, Tan X, Crosby K, Guimaraes AR, Upadhyay R, et al. Effective use of PI3K and MEK inhibitors to treat mutant Kras G12D and PIK3CA H1047R murine lung cancers. *Nat Med* 2008; 14:1351-6; PMID:19029981; <http://dx.doi.org/10.1038/nm.1890>
30. Doria-Rose VP, Sazabo E. Screening and prevention of lung cancer. In: Kernstine KH, RKL, ed(s). *Lung cancer: a multidisciplinary approach to diagnosis and management*. New York: Demos Medical Publishing, 2010:53-72
31. Siegel R, Ward E, Brawley O, Jemal A. Cancer statistics, 2011: the impact of eliminating socioeconomic and racial disparities on premature cancer deaths. *CA Cancer J Clin* 2011; 61:212-36; PMID:21685461; <http://dx.doi.org/10.3322/caac.20121>
32. Spetman B, Leuking S, Roberts B, Dennis JH. Microarray mapping of nucleosome position. In: Craig J, WN, ed(s). *Epigenetics: a reference manual*. Norwich, UK: Horizon Scientific Press, 2011:337-47